Reporter Metabolite Analysis of Transcriptional Profiles of a *Staphylococcus aureus* Strain with Normal Phenotype and Its Isogenic *hemB* Mutant Displaying the Small-Colony-Variant Phenotype[∇][†]

Jochen Seggewiß,[1] Karsten Becker,[1] Oliver Kotte,[2] Martin Eisenacher,[3] Mohammad Reza Khoschkhoi Yazdi,[1] Andreas Fischer,[1] Peter McNamara,[4] Nahed Al Laham,[1] Richard Proctor,[4] Georg Peters,[1] Matthias Heinemann,[2] and Christof von Eiff[1]*

Institute of Medical Microbiology, University of Münster, Münster, Germany[1]; Institute of Molecular Systems Biology, ETH Zürich, Zürich, Switzerland[2]; Integrated Functional Genomics (IFG), Interdisciplinary Center for Clinical Research (IZKF), University of Münster, Münster, Germany[3]; and Department of Medical Microbiology and Immunology, University of Wisconsin Medical School, Madison, Wisconsin[4]

In this study, full-genome DNA microarrays based on the sequence of *Staphylococcus aureus* N315 were used to compare the transcriptome of a clinical *S. aureus* strain with a normal phenotype to that of its isogenic mutant with a stable small-colony-variant (SCV) phenotype (*hemB::ermB*). In addition to standard statistical analyses, systems biology advances were applied to identify reporter metabolites and to achieve a more detailed survey of genome-wide expression differences between the *hemB* mutant and its parental strain. Genes of enzymes involved in glycolytic and fermentative pathways were found to be up-regulated in the *hemB* mutant. Furthermore, our analyses allowed identification of additional differences between the normal-phenotype *S. aureus* and the SCV, most of which were related to metabolism. Profound differences were identified especially in purine biosynthesis as well as in arginine and proline metabolism. Of particular interest, a hypothetical gene of the Crp/Fnr family (SA2424) that is part of the arginine-deiminase (AD) pathway, whose homologue in *Streptococcus suis* is assumed to be involved in intracellular persistence, showed significantly increased transcription in the *hemB* mutant. The *hemB* mutant potentially uses the up-regulated AD pathway to produce ATP or (through ammonia production) to counteract the acidic environment that prevails intracellularly. Moreover, genes involved in capsular polysaccharide and cell wall synthesis were found to be significantly up-regulated in the *hemB* mutant and therefore potentially responsible for the changed cell morphology of SCVs. In conclusion, the identified differences may be responsible for the SCV phenotype and its association with chronic and persistent infections.

The opportunistic pathogen *Staphylococcus aureus* is one of the major causes of nosocomial and community-acquired diseases that may range from superficial skin infections to life-threatening systemic infections and toxicoses (15). The ability of this species to cause such a wide spectrum of disease and to adapt to changing conditions is conferred by an impressive arsenal of pathogenicity and virulence factors that are globally regulated (3).

S. aureus may have an intrinsic ability for resisting treatment with antimicrobial agents that extends beyond what are now considered classical mechanisms of drug resistance (24). The discovery and characterization of a naturally occurring subpopulation of *S. aureus*, designated small-colony variants (SCVs), and their association with chronic and persistent infections have provided new insight into the understanding of the pathogenesis of *S. aureus* (26). Several studies showed that

SCVs, in contrast to their normal-phenotype parental strain progenitors, can be internalized by and persist within nonprofessional phagocytes (34–36). The capacity of SCVs to persist intracellularly and to hide within host cells can be regarded as a strategy of the bacteria for survival within the host and an additional strategy to evade antibiotic challenge and host defenses (26).

Clinical (i.e., genetically undefined) SCVs are frequently auxotrophic for hemin or menadione, two compounds involved in the synthesis of the electron carriers cytochrome and menaquinone, respectively, and exhibit a high rate of reversion to a normal, large-colony form. The genetic nature of the observed auxotrophies and the instability of the auxotrophic phenotype remain to be determined. To create a genetically and phenotypically stable SCV, a *hemB*-knockout mutant was created by allelic exchange (36). Genetically defined *S. aureus hemB* mutants have been compared with SCVs recovered from clinical specimens and have proved to exhibit the major characteristics of the SCV phenotype of clinical strains: slow growth, decreased pigment formation, resistance to aminoglycosides, low coagulase activity, and reduced hemolytic activity (1, 29, 30, 34, 36).

To provide a more complete analysis of SCV phenotypes

---

* Corresponding author. Mailing address: Institute of Medical Microbiology, University Hospital of Münster, Domagkstr. 10, 48149 Münster, Germany. Phone: 49-251-83-55360. Fax: 49-251-83-55350. E-mail: eiffc@uni-muenster.de.

and to gain a clearer insight into physiological changes that lead to in vivo antibiotic resistance and persistence, SCV mutants that reproduce the SCV phenotype were compared to their parental strain by various approaches. By application of a high-resolution two-dimensional protein gel electrophoresis technique coupled with matrix-assisted laser desorption ionization–time of flight mass spectrometry, proteins involved in the glycolytic pathway and in fermentation pathways were found to be induced in an exponentially growing *hemB* mutant compared to its wild-type parental strain (12). Again compared to the parent strain, phenotype microarray analysis of over 1,500 phenotypes revealed that a *hemB* mutant was defective in utilizing a variety of carbon sources including tricarboxylic acid (TCA) cycle intermediates and compounds that generate ATP via electron transport (37). Furthermore, hexose phosphates and other carbohydrates that provide ATP in the absence of electron transport stimulated growth of the *hemB* mutant compared to its wild-type parental precursor strain. Finally, based on a subgenomic DNA microarray analysis (i.e., 460 genes), it has been suggested that SigB might play a role in the expression of the SCV phenotype (19).

Despite these recent analyses of SCV phenotype and insights into the physiological differences between the normal phenotype and the SCV, we are still lacking an understanding of the signaling and regulatory mechanisms underlying the expression of the SCV phenotype of *S. aureus*. It is anticipated that identification of differences between the normal phenotype and SCV phenotype might provide clues into this circuitry. Here, genome-wide techniques offer unprecedented potential for identification of undiscovered phenotypic differences as these techniques screen on a system-wide level. In none of the previous studies was a complete analysis of genes differentially expressed in SCV and normal-phenotype *S. aureus* performed.

In this study, a comparative, genome-wide transcriptome analysis of an *S. aureus hemB* mutant displaying the clinical SCV phenotype versus the wild-type parental strain with normal phenotype was conducted. First, we employed a standard statistical analysis of the transcription data. Second, we harnessed the potential of recent systems biology advances to analyze the simple but notoriously overwhelming transcriptome data. We employed a recent genome-scale reconstruction of the *S. aureus* metabolic network (7) and a novel pathway-driven computational algorithm (20) to further extract metabolism-related transcriptional differences between the mutant and the parental strain.

MATERIALS AND METHODS

Bacterial strains and growth conditions. *S. aureus* wild-type strain A22223I, recovered from a fistula tract of a patient with chronic osteomyelitis and most recently used in a *Caenorhabditis elegans* infection model (30), and its isogenic *hemB* mutant (A22223I *hemB::ermB*), displaying the small-colony-variant phenotype, were used for all experiments. The strain A22223I was selected as the parent strain for the construction of the *hemB* mutant, because the strain was recovered in parallel with an *S. aureus* isolate displaying the SCV phenotype. As this hemin-auxotrophic SCV isolate revealed an unstable phenotype, exhibiting a high rate of reversion to the large-colony form, the isogenic parent strain A22223I was used to construct a genetically defined and stable SCV phenotype. This *hemB* mutant was constructed by allelic replacement with an *ermB* cassette-inactivated *hemB* gene, as previously described (34, 36). Furthermore, a complemented mutant with restored normal phenotype was constructed as previously reported (36). To keep the strains in a low passage number, strains were taken

from stored small aliquots. Overnight cultures in tryptic soy broth (TSB) medium (Becton Dickinson GmbH, Heidelberg, Germany) were inoculated with a single colony. In precultures (prior to RNA isolation), the *hemB* mutant was grown in TSB supplemented with erythromycin at a concentration of 2.5 μg/ml.

RNA isolation. For RNA isolation, shaking flasks (100 ml TSB in 500-ml flasks as used in a previous study [12]) were inoculated to an optical density at 578 nm of 0.05 into fresh TSB medium at 37°C and 160 rpm by using overnight cultures (15). Samples were collected and processed at least in triplicate to analyze at least three RNA samples for each strain and time point. Cells of the parent strain were harvested after 150, 270, 375, 480, and 600 min and cells of the *hemB* mutant after 240, 330, 390, 495, and 600 min, to provide bacteria in the same growth phase (Fig. 1) and as performed in a previous study (12). A volume of 10 ml of a bacterial suspension of the parent strain was immediately mixed with 10 ml of RNAprotect (QIAGEN, Hilden, Germany), vortexed for 5 s, incubated for 5 min at room temperature, and pelleted by centrifugation for 10 min at 4,000 × g. To compensate for the difference in cell number, 10 10-ml-volume suspensions of the *hemB* mutant were pelleted by centrifugation (10 min at 4,000 × g). Each pellet was immediately resuspended in 1 ml of RNAprotect (QIAGEN). Then, the 10 *hemB* mutant suspensions were pooled, vortexed for 5 s, incubated for 5 min at room temperature, and harvested by centrifugation (10 min at 4,000 × g). The pooled bacterial pellets were resuspended in 1 ml RNApro solution (Qbiogene, Heidelberg, Germany) and purified on a Matrix E column (Qbiogene). Cells were separated by mechanical lysis using a FastPrep Instrument (Qbiogene): once at 30 s, attitude of disruption 6.5, 30 s on ice, and once at 30 s, attitude 6.5. Further RNA purification was performed using the RNeasy Mini Kit (QIAGEN) according to the manufacturer's recommendations. Contaminating DNA in the RNA preparations was removed using DNase as described by the manufacturer (QIAGEN).

The RNA quality and quantity were determined by measurement of the absorbance at 260 and 280 nm (Eppendorf BioPhotometer; Hamburg, Germany) and agarose gel electrophoresis (intact rRNA bands). Purified RNA was stored at −70°C. Independent samples of RNA were used for each time point on separate microarrays.

cDNA synthesis, labeling, and microarray hybridization. *S. aureus* N315 microarrays were purchased from Scienion (Scienion AG, Berlin, Germany) and were produced by spotting 2,338 PCR products (of the 2,593 open reading frames [ORFs] of the annotated genome of *S. aureus* N315 [reference identification: NC_002745]) on a glass slide (details about the microarrays can be found at http://www.scienion.com). Each open reading frame was present in duplicate on the microarray. cDNA was synthesized from mRNA as recommended by the manufacturer of the microarray: RNA (12 μg unless otherwise indicated) from either A22223I or its *hemB* mutant was mixed with 1 μg of random hexamer primer (Invitrogen, Karlsruhe, Germany), 1 μl of RNase OUT (Invitrogen), and RNase-free water up to a volume of 10 μl. The samples were denatured at 70°C for 10 min and then cooled on ice for 1 min. Labeled cDNA was synthesized by mixing the denatured RNA with 200 U of Superscript III reverse transcriptase (Invitrogen), Cy3- and Cy5-dUTP, deoxynucleoside triphosphate mix, and appropriate buffer in a reaction mix according to the manufacturer's protocol (Scienion). The mixture was incubated for 10 min at 25°C, followed by incubation at 47°C for 60 min. Two hundred units of Superscript III reverse transcriptase (Invitrogen) was added again, followed by a further incubation for 40 min at 47°C. The reaction was stopped by adding 5 μl of 500 mM EDTA. Then, the mixture was incubated for 15 min at 65°C after NaOH (5 μl, 1 M) was added to hydrolyze the RNA. The sample was neutralized with 12.5 μl of Tris-HCl (1 M, pH 7.5), and the resulting cDNA was purified using a QIAquick PCR purification kit (QIAGEN). The volumes of the labeled cDNA solutions were reduced to 3 μl by using a SpeedVac (Thermo Electron Corp., Waltham, MA). The Cy3- and Cy5-labeled cDNA solutions were mixed, resuspended in 49 μl of prewarmed (48°C) hybridization solution (Scienion), and incubated for 5 min at 48°C. The mixture of labeled products was denatured for 2 min at 95°C. The combined samples were hybridized to the *S. aureus* N315 microarrays for 72 h at 48°C. The slides were washed according to the manufacturer's protocol and stored at −70°C. For each of the five time points, at least three DNA microarrays plus one dye-switch experiment (to check cDNA synthesis and labeling) were analyzed.

Data analysis. The hybridized microarrays were scanned with a GMS418 array scanner (Affymetrix, Santa Clara, CA). A geometric raster was laid over the resulting microarray picture to distinguish the signals from the background. After localization of single spots, the spot intensities and the global background were calculated.

The hybridization patterns and intensities were quantitatively analyzed using the Imagene 6 software (BioDiscovery, El Segundo, CA). The replicates were averaged, and the spots identified by Imagene 6 as flawed were omitted. The data set was normalized by application of the LOWESS algorithm. The data from
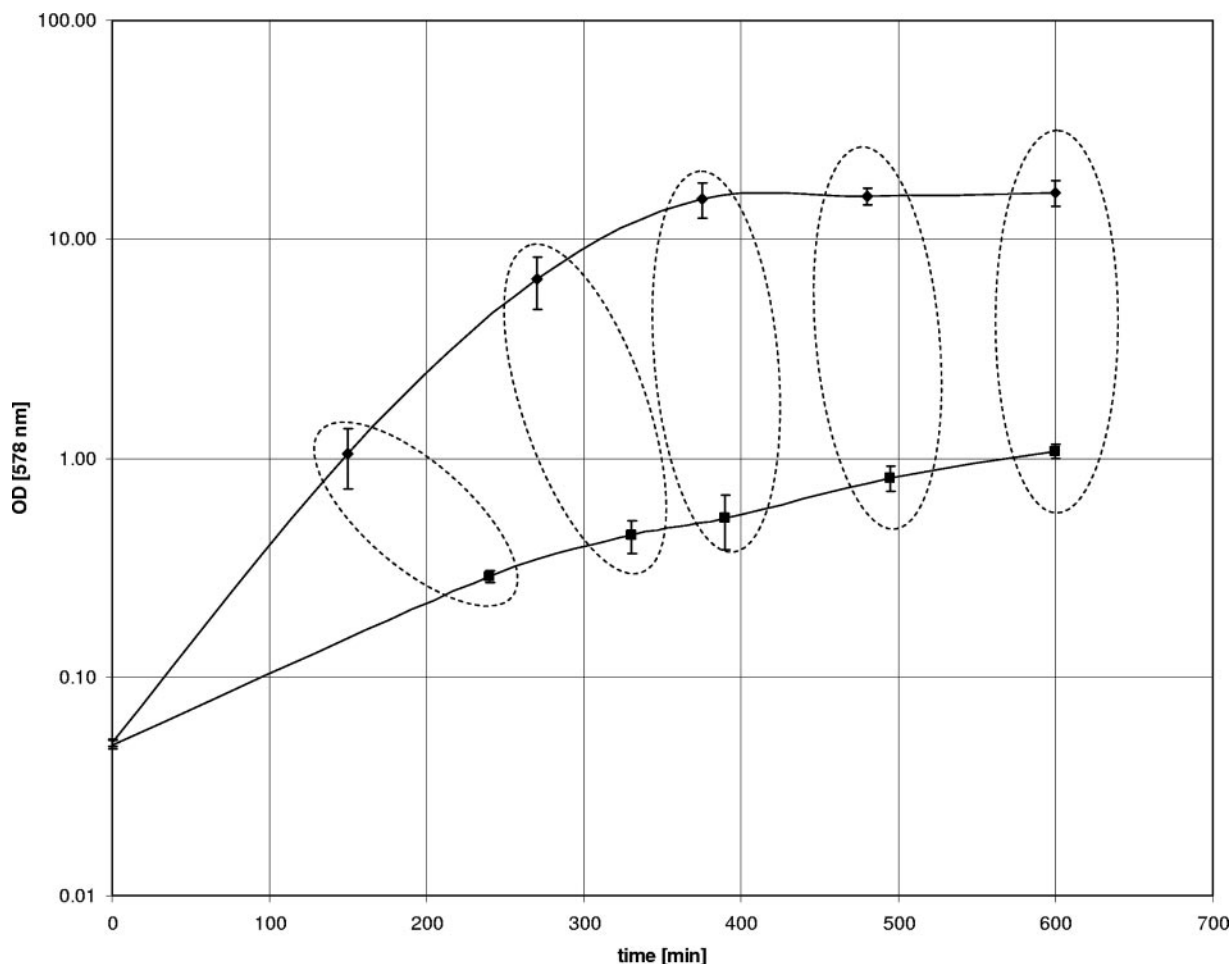
FIG. 1. Growth of the *S. aureus* A22223I parental wild-type strain (◆) and its isogenic *hemB* mutant (■) in TSB (with standard deviations). The times of sampling for transcriptional analysis are indicated by the symbols on the growth curves. Time points for RNA isolation were selected as previously described (12). Optical density was measured at 578 nm.

Imagene 6 were exported into Expressionist (GeneData, Basel, Switzerland) and Excel (Microsoft Corporation, Redmond, WA) software for further analysis as, e.g., identification of microarrays that present technical outliers. The expression intensities of one single array, resulting from multiple scans with different gains, were averaged. In a next step, the averaged intensity values of all arrays for each time point as well as for all time points combined were used for *t* tests. Genes with a change of <0.4- or ≥2.0-fold were characterized as having significantly differing amounts of transcripts based on *t* tests with a *P* value cutoff of at least 0.05. Gene functions were assigned to the respective accession numbers and annotations as compiled on DOGAN, a web page for *S. aureus* N315 (http://www.bio.nite.go.jp/dogan/MicroTop?GENOME_ID=n315G1). Fisher's exact test was used to decide whether functional annotations show a tendency of over- or underrepresentation in a candidate gene list compared to all measured and annotated items.

The microarray data were also analyzed by a recently developed algorithm that uses the topology of an organism's metabolic network to uncover underlying metabolism-related transcriptional regulation (20). This algorithm first converts a genome-scale metabolic network (we employed the recently reconstructed genome-scale metabolic network of *S. aureus* N315 [7]) into a bipartite metabolic graph. In this graph, each metabolite node is then scored based on the normalized transcriptional response of its neighboring enzymes. Using the genes' *P* values as inputs to score the enzyme nodes, the algorithm identifies so-called reporter metabolites, designating metabolites around which the most significant transcriptional changes occur. The mapping of transcription data onto a metabolic network, which underlies the employed algorithm, allows identifying spots (so-called reporter metabolites) around which significant regulation occurs and thus assists in carving out metabolism-related insight from the microarray data.

Validation of array data by real-time PCR. To determine the validity of the array data, selected transcriptional changes obtained with the microarray analysis were compared with those from quantitative real-time PCR. For a list of the genes and primer sequences used for the real-time PCR analysis, see Table S1 in the supplemental material. The real-time PCR was performed by using the iCycler (Bio-Rad Laboratories GmbH, Munich, Germany) with a QuantiTect reverse transcription kit (QIAGEN) and the DyNAmo HS SYBR Green qPCR Kit (Finnzymes Oy, Espoo, Finland). Reaction mixtures were initially incubated for 15 min at 95°C, followed by 40 cycles of 15 s at 95°C, 30 s at 55.0°C, and 30 s at 72°C. PCR efficiencies were derived from standard curve slopes in the iCycler software v. 3.0a (Bio-Rad Laboratories). The expression rates were calculated using Gene Expression Analysis for iCycler iQ Real-Time PCR Detection System v1.10 (Bio-Rad Laboratories). Melting-curve analysis was also performed to evaluate PCR specificity and resulted in single, primer-specific melting temperatures.

RESULTS AND DISCUSSION

SCVs recovered from clinical specimens are frequently auxotrophic for hemin. For *S. aureus*, in vitro gentamicin-selected SCVs are found that carry mutations in the *hem* operon, which encodes enzymes required for hemin biosynthesis (28). Furthermore, an *Escherichia coli* SCV has been isolated from a patient and has been shown to carry a *hemB* mutation that renders the bacterium defective in hemin bio-

TABLE 1. Validation of array data by real-time PCR[a]

Gene identifier	Gene	Quantitative real-time RT-PCR[b] result (relative difference in expression change)			Expression difference of the *hemB* mutant analyses compared to the wild type using microarrays[c]
		hemB mutant	Complemented mutant	Wild type	
SA0150	Capsular polysaccharide synthesis enzyme Cap5G	29.9	1.1	1.0	Sig. up-reg.
SA0232	L-Lactate dehydrogenase	21.1	1.0	1.2	Sig. up-reg.
SA0742	Fibrinogen-binding protein A	494.6	12.6	1.0	Sig. up-reg.
SA0922	Phosphoribosylpyrophosphate amidotransferase PurF	1.0	24.3	10.6	Sig. down-reg.
SA1141	Glycerol kinase	40.8	3.6	1.0	Sig. up-reg.
SA1142	Aerobic glycerol-3-phosphate dehydrogenase	128.0	1.0	2.4	Sig. up-reg.
SA2206	Immunoglobulin G-binding protein SBI	1.0	4.3	8.3	Sig. down-reg.
SA2424	Hypothetical protein, similar to transcription regulator Crp/Fnr family protein	163.1	1.0	1.3	Sig. up-reg.
SA2426	Arginine/ornithine antiporter	891.0	1.0	1.3	Sig. up-reg.
SA2428	Arginine deiminase	989.0	2.1	1.0	Sig. up-reg.

[a] Transcription rates of selected genes for the *S. aureus hemB* mutant in comparison to the wild type and the complemented mutant for pooled time points. The relative differences in expression change were calculated using Gene Expression Analysis for iCycler iQ Real-Time PCR Detection System v1.10 (Bio-Rad). The lowest expression was set to 1.0. *gyrA* (SA0006) was used as a housekeeping gene for relative quantification.
[b] RT-PCR, reverse transcription-PCR.
[c] See Table 2. Abbreviations: sig. up-reg., significantly up-regulated; sig down-reg., significantly down-regulated.

synthesis (27). In this study, a stable genetically defined *S. aureus* SCV *hemB* mutant was employed to serve as a model organism for the transcriptional changes that occur upon loss of hemin biosynthesis. The model organism was used to limit the uncertainty associated with using an undefined genetic background and reversible phenotypes found in genetically undefined clinical SCVs and gentamicin-induced SCVs (36). Past studies using defined *S. aureus hemB* mutants, in part in comparison with clinical SCVs, had previously shown that this organism confers the major features of the SCV phenotype (1, 9, 12, 29, 30, 34, 36, 37).

Transcriptional differences between the *S. aureus hemB* mutant and its parent strain. In this study, the *hemB* mutant displaying the SCV phenotype was applied on a full-genome microarray to get a complete view of the transcriptional profile of SCVs. More specifically, we compared the expression levels of the *S. aureus hemB* mutant and its parent strain at five time points, corresponding to different growth phases: lag phase, early exponential phase, mid-exponential phase, late exponential phase, and stationary phase (Fig. 1).

To verify the microarray data, quantitative real-time reverse transcription-PCR studies were performed for selected genes of the *S. aureus* parent strain, its *hemB* mutant, and its complemented mutant. In fact, the results of quantitative real-time reverse transcription-PCR analyses of selected transcripts were found to be in excellent accordance with the microarray analysis. This was true for the pooled time points (Table 1) as well as for the single time points (data not shown).

With the standard statistical analysis of the acquired genome-wide transcription data, when values from different growth phases were pooled, 170 genes were found to be significantly changed when the wild-type and the *hemB*-disrupted strains were compared. Compared to the parent strain, 48 of these genes were significantly down-regulated and 122 genes were significantly up-regulated in the *hemB* mutant. All significantly differently expressed genes in the combined analysis of all values from all growth phases are listed in Table 2. Data from each phase of growth are listed in Tables S2 to S6 in the supplemental material. To reveal functional groups of genes

that are in general differentially expressed in the *hemB* mutant compared to the parent strain, we performed Fisher's exact test using the classification from the DOGAN web page (results are shown in Table 3).

As demonstrated in past studies, the phenotype of the *hemB* mutant is characterized by a significantly reduced growth rate and an excretion of lactate instead of acetate, both giving indication of metabolic differences between the mutant and its parental strain. In fact, recent proteomic and phenotypic microarray studies underlined the significance of metabolic differences, such as the defect of the *hemB* mutant in utilization of a variety of carbon sources, including TCA cycle intermediates and compounds that ultimately generate ATP via electron transport. Furthermore, hexose phosphates and other carbohydrates that provide ATP in the absence of electron transport were found to stimulate growth of the *hemB* mutant (12, 37). Thus, besides the standard statistical analysis we put a special focus on metabolism-related transcriptional changes by using a recently developed algorithm from systems biology (20).

Before using this algorithm, we first extracted the genes from the microarray data that are related to metabolic functions. For this, we employed the recently reconstructed *S. aureus* metabolic network (7), leaving us with approximately 560 genes that encode enzymes where substrates and products are known. In a next step, we used the computational method of Patil and Nielsen (20) to computationally map the transcriptional changes of this set of genes onto the metabolic network (cf. Materials and Methods). Thus, by this linking of transcription data with metabolism (in contrast to an otherwise isolated analysis of single genes) the transcriptional changes in the *hemB* mutant (compared to its wild-type strain) were considered in a metabolic context. In fact, this approach enables a condensation of transcriptional data to a number of metabolites around which substantial transcriptional changes occur. Patil and Nielsen called these metabolites "reporter metabolites" (20) as they mark spots in the metabolism around which regulation occurs most likely in order to either increase, decrease, or redirect a metabolic flux. In a broader view, com-

TABLE 2. Genes differently expressed in the *S. aureus hemB* mutant for combined values over the whole time course (0 to 10 h)

Function group and ORF (N315)	P value by t test[a]	Fold change[b]	Description
Adaptation to atypical conditions			
SA0147	0.00	3.16	Capsular polysaccharide synthesis Cap5D
SA0144	0.00	3.60	Capsular polysaccharide synthesis Cap5A
SA1549	0.00	2.64	Hypothetical protein similar to serine proteinase Do heat shock protein HtrA
SA0145	0.00	2.65	Capsular polysaccharide synthesis Cap5B
SA2494	0.00	3.05	Cold shock protein
SA1096	0.00	2.23	Heat shock protein
SA0146	0.00	2.89	Capsular polysaccharide synthesis Cap8C
SA2336	0.00	2.30	ATP-dependent Clp proteinase chain ClpL
SA0148	0.01	2.60	Capsular polysaccharide synthesis Cap8E
SA0150	0.03	2.04	Capsular polysaccharide synthesis Cap5G
SA0149	0.03	2.14	Capsular polysaccharide synthesis Cap5F
Antibiotic production			
SA0173	0.01	2.19	Hypothetical protein similar to surfactin synthetase
Cell wall			
SA1691	0.00	3.52	Hypothetical protein similar to protein 1A/1B
SA1283	0.00	2.14	Penicillin-binding protein 2
SA1024	0.00	2.32	Penicillin-binding protein 1
Membrane bioenergetics (electron transport chain and ATP synthase)			
SA0411	0.00	5.00	NADH dehydrogenase subunit
SA0211	0.00	0.10	Hypothetical protein similar to NADH-dependent dehydrogenase
SA0210	0.00	0.13	Hypothetical protein similar to NADH-dependent dehydrogenase
SA0366	0.00	0.38	Alkyl hydroperoxide reductase C
SA0938	0.01	2.13	Cytochrome *d* ubiquinol oxidase subunit II homologue
SA1132	0.02	2.34	Hypothetical protein similar to ferredoxin oxidoreductase beta subunit
SA0937	0.02	2.14	Cytochrome *d* ubiquinol oxidase subunit I homologue
SA1311	0.02	2.12	Hypothetical protein similar to thioredoxin reductase homologue
SA1315	0.03	2.31	Ferredoxin
Metabolism of amino acids and related molecules			
SA2428	0.00	4.96	Arginine deiminase
SA2341	0.00	0.38	1-Pyrroline-5-carboxylate dehydrogenase
SA1165	0.00	0.39	Threonine synthase
SA1166	0.00	0.39	Homoserine kinase homologue
SA0419	0.01	2.13	Cystathionine gamma-synthase
SA0416	0.01	2.05	Hypothetical protein similar to carboxylesterase
SA2427	0.02	4.24	Ornithine transcarbamoylase
SA2389	0.03	2.06	Truncated hypothetical protein similar to metalloproteinase Mpr precursor
Metabolism of carbohydrates and related molecules			
SA1142	0.00	5.46	Aerobic glycerol-3-phosphate dehydrogenase
SA0945	0.00	0.35	Dihydrolipoamide *S*-acetyltransferase component of pyruvate dehydrogenase complex E2
SA1245	0.00	0.20	2-Oxoglutarate dehydrogenase E1
SA2008	0.00	3.40	Alpha-acetolactate synthase
SA0730	0.00	2.38	Phosphoglycerate mutase
SA1184	0.00	0.34	Aconitate hydratase
SA1244	0.00	0.26	Dihydrolipoamide succinyltransferase
SA1141	0.00	2.57	Glycerol kinase
SA0728	0.00	2.43	Phosphoglycerate kinase
SA2007	0.00	2.68	Hypothetical protein similar to alpha-acetolactate decarboxylase
SA0729	0.00	2.16	Triosephosphate isomerase
SA0182	0.00	0.36	Hypothetical protein similar to indole-3-pyruvate decarboxylase
SA1553	0.00	0.33	Formyltetrahydrofolate synthetase
SA1089	0.00	0.38	SucD succinyl coenzyme A synthetase alpha chain
SA2327	0.00	2.27	Hypothetical protein similar to pyruvate oxidase
SA1554	0.00	0.30	Acetyl coenzyme A synthetase
SA0232	0.00	40.16	L-Lactate dehydrogenase
SA0219	0.01	2.22	Formate acetyltransferase activating enzyme

TABLE 2—*Continued*

Function group and ORF (N315)	*P* value by *t* test[a]	Fold change[b]	Description
SA0654	0.02	2.40	Fructose 1-phosphate kinase
SA1517	0.02	0.39	Isocitrate dehydrogenase
Metabolism of coenzymes and prosthetic groups			
SA1492	0.00	2.06	Delta-aminolevulinic acid dehydratase
Metabolism of nucleotides and nucleic acids			
SA0923	0.00	0.22	Phosphoribosylformylglycinamidine cycloligase PurM
SA0924	0.00	0.23	Phosphoribosylglycinamide formyltransferase
SA0921	0.00	0.24	Phosphoribosylformylglycinamidine synthetase PurL
SA0922	0.00	0.26	Phosphoribosylpyrophosphate amidotransferase PurF
SA0916	0.00	0.28	Hypothetical protein similar to phosphoribosylaminoimidazole carboxylase PurE
SA0925	0.00	0.27	Bifunctional purine biosynthesis PurH
SA0920	0.00	0.34	Phosphoribosylformylglycinamidine synthase II
SA2297	0.00	2.63	Hypothetical protein similar to GTP-pyrophosphokinase
SA0373	0.00	0.32	Xanthine phosphoribosyltransferase
SA0918	0.01	0.39	Phosphoribosylaminoimidazolesuccinocarboxamide synthetase homologue
Metabolism of phosphate			
SA2301	0.00	2.27	Hypothetical protein similar to alkaline phosphatase
No similarity			
SA2221	0.00	3.60	Hypothetical protein
SA1476	0.00	5.66	Hypothetical protein
SA2011	0.00	4.10	Hypothetical protein
SA2272	0.00	2.05	Hypothetical protein
SA1774	0.00	2.29	(Bacteriophage phiN315) hypothetical protein
SA0536	0.00	3.20	Hypothetical protein
SA2091	0.00	0.26	Hypothetical protein
SA1773	0.00	2.26	(Bacteriophage phiN315) hypothetical protein
SA1772	0.00	2.48	(Bacteriophage phiN315) hypothetical protein
SA1703	0.00	3.22	Hypothetical protein
SA0535	0.01	2.47	Hypothetical protein
SA0885	0.02	2.12	Hypothetical protein
SA2113	0.03	2.25	Hypothetical protein
SAS014	0.03	2.22	Hypothetical protein
SA2268	0.04	2.16	Hypothetical protein
Pathogenic factors (toxins and colonization factors)			
SA0587	0.00	0.13	Lipoprotein streptococcal adhesin PsaA
SA2430	0.00	2.37	Zinc metalloproteinase aureolysin
SA2206	0.00	0.29	Immunoglobulin G-binding protein SBI
SA0390	0.00	3.81	(Pathogenicity island SaPIn2) 14
SA2097	0.01	2.68	Hypothetical protein similar to secretory antigen precursor SsaA
SA0742	0.01	2.14	Fibrinogen-binding protein A
SA2356	0.02	2.12	Immunodominant antigen A
Phage-related functions			
SA1796	0.00	6.74	(Bacteriophage phiN315) hypothetical protein
SA1782	0.00	2.86	(Bacteriophage phiN315) hypothetical protein
SA1785	0.00	2.04	(Bacteriophage phiN315) hypothetical protein
SA1783	0.01	2.38	(Bacteriophage phiN315) hypothetical protein
SA1788	0.02	2.03	(Bacteriophage phiN315) hypothetical protein
SA1775	0.02	2.31	(Bacteriophage phiN315) hypothetical protein
SA1797	0.02	2.12	(Bacteriophage phiN315) hypothetical protein
Protein folding			
SA1659	0.00	2.89	Peptidyl-prolyl *cis/trans* isomerase homologue
RNA modification			
SA1713	0.02	2.10	RNA methyltransferase homologue
SA1885	0.02	2.13	Hypothetical protein similar to RNA helicase
RNA synthesis			
SA2424	0.00	9.18	Hypothetical protein similar to transcription regulator Crp/Fnr family protein

TABLE 2—*Continued*

Function group and ORF (N315)	*P* value by *t* test[a]	Fold change[b]	Description
SA2092	0.00	0.20	Hypothetical protein similar to transcription regulator
SA1949	0.00	4.15	Lytic regulatory protein truncated with Tn*554*
SA1956	0.00	3.35	Lytic regulatory protein truncated with Tn*554*
SA1700	0.00	4.09	Two-component response regulator
SA2429	0.00	3.61	Hypothetical protein similar to arginine repressor
SA0108	0.00	0.30	Staphylococcal accessory regulator A
SA2296	0.00	2.71	Hypothetical protein similar to transcriptional regulator MerR family
SA2103	0.00	2.20	Hypothetical protein similar to divergon expression attenuator LytR
SA1139	0.00	2.11	Glycerol uptake operon regulatory protein
SA0653	0.00	2.82	Hypothetical protein similar to repressor of fructose operon
SA1961	0.00	2.26	Hypothetical protein similar to transcription antiterminator BglG family
SA2418	0.01	2.18	Hypothetical protein similar to response regulator
SA0187	0.01	0.39	Hypothetical protein similar to transcription regulator
SA2295	0.03	2.65	Gluconate operon transcriptional repressor
SA2287	0.03	2.06	Staphylococcal accessory regulator A
Sensors (signal transduction)			
SA1701	0.00	4.09	Two-component sensor histidine kinase
SA1653	0.00	2.03	Signal transduction protein
SA2417	0.01	2.15	Hypothetical protein similar to sensor histidine kinase
Similar to unknown proteins			
SA0175	0.00	5.39	Conserved hypothetical protein
SA1702	0.00	3.31	Conserved hypothetical protein
SA0412	0.00	5.20	Conserved hypothetical protein
SA0213	0.00	0.23	Conserved hypothetical protein
SA2220	0.00	3.26	Conserved hypothetical protein
SA0413	0.00	2.83	Conserved hypothetical protein
SA0212	0.00	0.14	Conserved hypothetical protein
SA0588	0.00	0.13	Conserved hypothetical protein
SA2329	0.00	3.96	Conserved hypothetical protein
SA1712	0.00	3.19	Conserved hypothetical protein
SA0908	0.00	3.66	Conserved hypothetical protein
SA2146	0.00	2.72	TcaA protein
SA0919	0.00	0.31	Conserved hypothetical protein
SA0725	0.00	2.75	Conserved hypothetical protein
SA1021	0.00	2.33	Conserved hypothetical protein
SA1031	0.00	2.67	Conserved hypothetical protein
SA1032	0.00	2.17	Conserved hypothetical protein
SA0824	0.00	2.29	Conserved hypothetical protein
SA1433	0.01	0.37	Conserved hypothetical protein
SA0301	0.01	0.40	Conserved hypothetical protein
SA0962	0.01	2.08	Conserved hypothetical protein
SA1033	0.02	2.38	Conserved hypothetical protein
SA2481	0.02	2.23	Conserved hypothetical protein
SA0415	0.02	2.16	Conserved hypothetical protein
SA2298	0.03	2.01	Conserved hypothetical protein
SA0174	0.04	2.01	Conserved hypothetical protein
SA1071	0.04	2.02	Conserved hypothetical protein
Transport/binding proteins and lipoproteins			
SA2426	0.00	16.29	Arginine/ornithine antiporter
SA0541	0.00	4.96	Hypothetical protein similar to amino acid transporter
SA1140	0.00	5.59	Glycerol uptake facilitator
SA1960	0.00	3.85	PTS mannitol-specific IIBC component
SA0293	0.00	3.77	Hypothetical protein similar to formate transporter NirC
SA2156	0.00	3.72	Permease LctP homologue
SA0589	0.00	0.11	Hypothetical protein similar to ABC transporter ATP-binding protein
SA2303	0.00	0.21	Hypothetical protein similar to membrane-spanning protein
SA0208	0.00	0.13	Maltose/maltodextrin transport permease homologue
SA2302	0.00	0.31	Hypothetical protein similar to ABC transporter
SA0111	0.00	0.38	Lipoprotein
SA0848	0.00	0.35	Oligopeptide transport system ATP-binding OppF homologue
SA2167	0.00	2.69	PTS sucrose-specific component
SA0207	0.00	0.21	Hypothetical protein similar to maltose/maltodextrin-binding protein
SA0849	0.00	0.35	Hypothetical protein similar to binding protein OppA

TABLE 2—*Continued*

Function group and ORF (N315)	P value by t test[a]	Fold change[b]	Description
SA0432	0.00	2.52	PTS enzyme II, phosphoenolpyruvate dependent, trehalose specific
SA0209	0.00	0.20	Maltose/maltodextrin transport permease homologue
SA0206	0.00	0.20	Multiple sugar-binding transport protein
SA0640	0.00	2.01	Hypothetical protein similar to ABC transporter required for expression of cytochrome *bd*
SA0172	0.00	2.19	Hypothetical protein similar to membrane protein LmrP
SA0186	0.00	0.38	Hypothetical protein similar to phosphotransferase enzyme II
SA0639	0.01	2.04	Hypothetical protein similar to ABC transporter required for expression of cytochrome *bd*
SA0531	0.01	2.20	Proline/betaine transporter homologue
SA0417	0.01	2.15	Hypothetical protein similar to sodium-dependent transporter
SA0655	0.01	2.25	Fructose-specific permease
SA0374	0.01	0.39	Xanthine permease
SA2053	0.01	2.06	Glucose uptake protein homologue
SA2434	0.02	2.31	Fructose phosphotransferase system enzyme homologue

[a] Only ORFs with a P value by t test of <0.05 have been listed.
[b] Only ORFs with a fold change of <0.4 or ≥2.0 for the *hemB* mutant versus the parent strain have been listed.

bined with information on the submetabolisms in which these metabolites occur, areas of significant regulatory action can be identified.

We first determined the reporter metabolites from *P* values obtained when the microarrays from all the different time points were combined. One of the top-scoring reporter metab-

olites that were identified in this combined analysis was 5-amino-levulinate, an intermediate in the synthesis of the electron transporter heme. It is synthesized from glutamate-1-semial-dehyde 2,1-aminomutase (encoded by *hemL*, SA1491) and further metabolized by aminolevulinic acid dehydratase (encoded by *hemB*, SA1492). The appearance of 5-aminolevulinate

TABLE 3. Results of Fisher's exact test showing overrepresented groups of genes in the *hemB* mutant at different growth phases

Time when group is overrepresented and group name	Group size (total size = 2,322)	Selection group size	Selection size	P value[a]
Pooled values of the whole time course			337	
Metabolism of carbohydrates and related molecules	133	34		0.00
Membrane bioenergetics (electron transport chain and ATP synthase)	54	17		0.00
Transport/binding proteins and lipoproteins	256	53		0.00
Metabolism of nucleotides and nucleic acids	74	18		0.02
Phage-related functions	43	11		0.04
Adaptation to atypical conditions	44	11		0.04
Lag phase			279	
Protein synthesis	85	25		0.00
Metabolism of nucleotides and nucleic acids	74	22		0.00
Metabolism of carbohydrates and related molecules	133	27		0.00
Adaptation to atypical conditions	44	12		0.00
Early logarithmic phase			171	
Metabolism of carbohydrates and related molecules	133	27		0.00
Transport/binding proteins and lipoproteins	256	34		0.00
Adaptation to atypical conditions	44	7		0.04
Logarithmic phase			113	
Metabolism of carbohydrates and related molecules	133	19		0.00
Metabolism of nucleotides and nucleic acids	74	10		0.00
Transport/binding proteins and lipoproteins	256	21		0.01
Early stationary growth phase			189	
Membrane bioenergetics (electron transport chain and ATP synthase)	54	13		0.00
Metabolism of carbohydrates and related molecules	133	20		0.00
Transport/binding proteins and lipoproteins	256	31		0.01
Stationary growth phase			46	
Membrane bioenergetics (electron transport chain and ATP synthase)	54	8		0.00
Protein synthesis	85	7		0.00
Metabolism of carbohydrates and related molecules	133	6		0.04

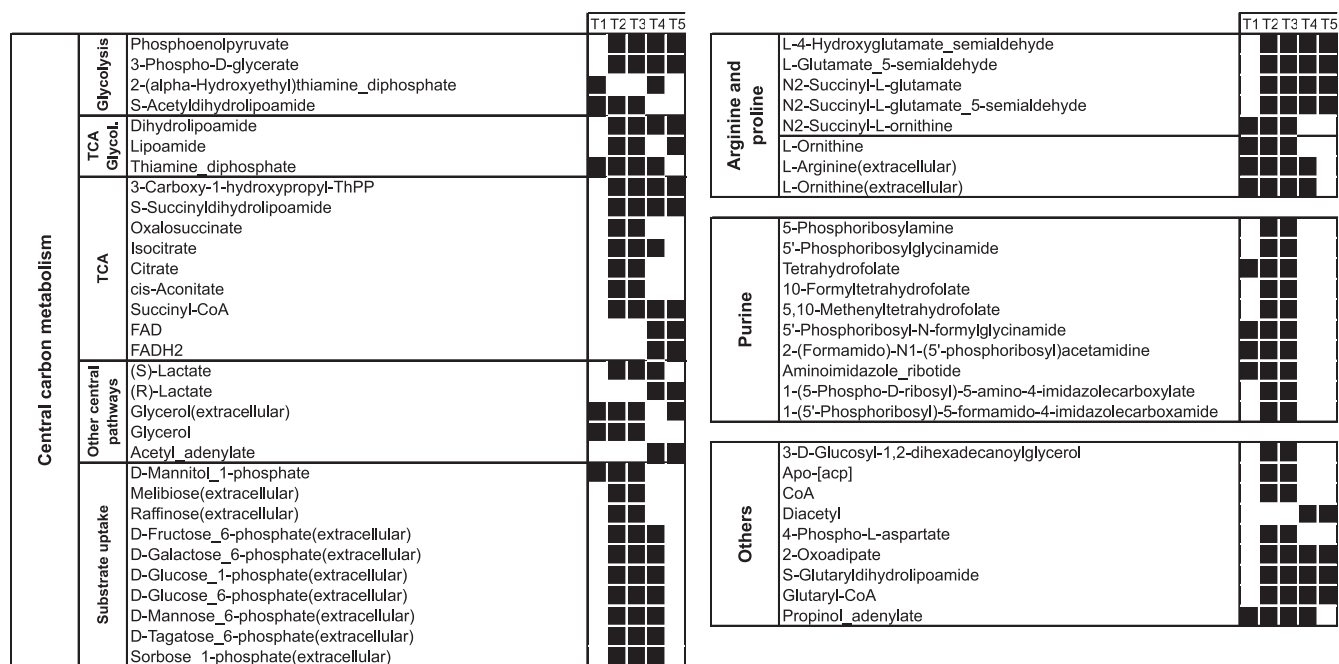[a] Only groups that are overrepresented are listed.

FIG. 2. Clustered top-scoring reporter metabolites (*P* values < 0.05) which occurred at more than one time point. Black boxes denote time points when the respective metabolite that occurred was identified as significant. CoA, coenzyme A; FAD, flavin adenine dinucleotide; FADH₂, reduced flavin adenine dinucleotide.

might be explained by the following two possibilities: (i) the up-regulation of *hemL* is an effect of the *hemB* knockout on expression from a distal promoter and, thus, most likely from the promoter of the *hem* operon (*hemAXCDBL*), or (ii) it is an effect resulting from the *erm* promoter: only *hemL* (SA1491) and *hemB* (SA1492) were found to be up-regulated whereas none of the other *hem* genes that belong to the *hem* operon (*hemAXCD*) showed a changed transcription profile. This led to the assumption that the change in transcription level is an effect of the *erm* promoter, which is indeed located upstream of *hemL* and upstream of the part of *hemB* spotted on the microarray. Therefore, it is assumed that the observed changes are an effect of the *erm* promoter. In any case, the occurrence of 5-aminolevulinate as a reporter metabolite provides evidence that the employed pathway-driven analysis of microarray data is able to uncover areas of regulatory action.

In the combined analysis of all time points, it was further found that most of the significant reporter metabolites (*P* < 0.05) cluster in three distinct metabolic regions: central carbon metabolism, arginine and proline metabolism, and purine synthesis (see Fig. S1 in the supplemental material). Below, we will focus our discussion on these areas.

Arginine and proline metabolism. The mutation in *hemB* led to an identification of L-arginine, L-arginine (extracellular), and L-ornithine (extracellular) as reporter metabolites, which are all involved in the arginine-deiminase (AD) pathway. The gene for the arginine/ornithine antiporter, *arcD* (SA2426), showed a 16.29-fold-higher expression in the combined analysis compared to the parent strain (Table 2). This reflects a significant difference between the *hemB* mutant and its parental strain. Similar changes were found for *arcA* (arginine de-

iminase, SA2428, 4.96-fold up-regulated) and *arcB* (ornithine transcarbamoylase, SA2427, 4.24-fold up-regulated).

The *hemB* mutant may regulate the AD pathway through a Crp/Fnr family transcriptional regulator. Fnr family regulators have previously been linked to AD system regulation (16, 17, 31), and they have proven to be responsible for anaerobic gene regulation in many gram-negative and some gram-positive bacteria (6, 12, 31). Particularly in *Streptococcus suis*, it has been shown that the AD system is induced under microaerophilic and anaerobic conditions (6). In accordance with the observations in *S. suis*, the *S. aureus* gene SA2424 product, a hypothetical protein similar to the transcription regulator from the Crp/Fnr family, was up-regulated in the *hemB* mutant (9.18-fold, pooled values for all five time points) in comparison with the parent strain, and it might play an important role in the regulation of the AD pathway.

It was demonstrated that the AD system can be considered a system that protects streptococci against acidic stress (2, 4), a trait that would correlate with the ability of SCVs to persist intracellularly (36). It may be assumed that the up-regulated AD system allows *S. aureus* SCVs to counteract (through ammonia production) the intracellular acidic environment. However, it is also conceivable that the *hemB* mutant uses this pathway to produce ATP as was hypothesized in previous studies (7, 12).

Also from the arginine and proline metabolism, another set of reporter metabolites was identified (L-4-hydroxyglutamate semialdehyde, L-glutamate 5-semialdehyde, N_2-succinyl-L-glutamate, and N_2-succinyl-L-glutamate 5-semialdehyde). The genes whose products act on these metabolites are *rocA* (SA2341) and *rocD* (SA0181), which are both down-regulated
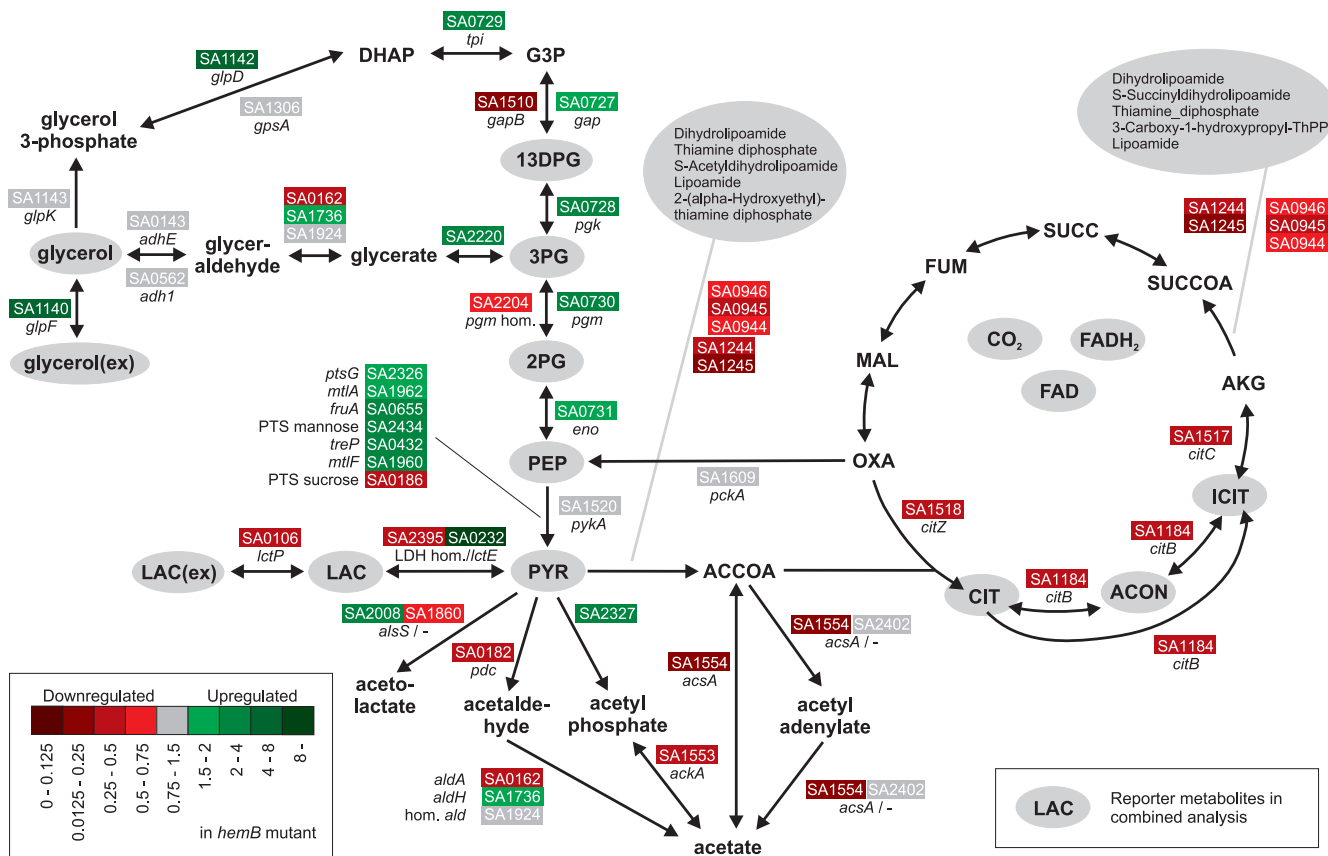
FIG. 3. Illustration of significant transcriptional changes in the context of metabolic pathways of central carbon metabolism based on the combined analysis of all time points. Metabolites in gray circles denote reporter metabolites (*P* values < 0.05). Gene names are given in italics. A gene's down-regulation in the *hemB* mutant compared to the parental strain is indicated by a red box around the gene locus (based on the *S. aureus* N315 sequence), and a gene's up-regulation is indicated by a green box. Dark colors denote strong down- and up-regulation. PEP, phosphoenolpyruvate; FAD, flavin adenine dinucleotide; FADH₂, reduced flavin adenine dinucleotide.

in the *hemB* mutant compared to its wild-type progenitor strain. From the analysis of data collected from each phase of bacterial growth (Fig. 2), significant changes are evident only at the second through the fifth time point. These genes are involved in arginine catabolism, where arginine is cleaved by arginase to give ornithine, which is converted to glutamate semialdehyde by ornithine aminotransferase (*rocD* gene product). Finally, the conversion of glutamate semialdehyde to glutamate is catalyzed by the *rocA* gene product. The *roc* pathway is generally considered an aerobic pathway for the metabolism of L-arginine that terminates in L-glutamate (17, 18). Potentially, the down-regulation of *rocA* and *rocD* prevents a drain of ornithine towards glutamate, which in turn would result in a lower efficiency of the AD pathway to counteract acidic conditions or provide ATP.

Central carbon metabolism. We identified a large number of metabolites from central carbon metabolism as reporter metabolites. More specifically, these metabolites belong to the terminal part of glycolysis, glycerol metabolism, pyruvate metabolism, and acetate metabolism and to the TCA cycle (Fig. 2 and 3).

The significant changes in glycolysis on one hand were caused by an up-regulation of an operon consisting of SA0727, SA0728, SA0730, and SA0731 and on the other hand by a

significant down-regulation of genes encoding two sets of isoenzymes (SA1510 [homologous to SA0727] and SA2204 [homologous to SA0730]) (Fig. 3).

Genes encoding products responsible for the metabolism of glycerol showed significantly increased expression levels in the *hemB* mutant (Fig. 3): glycerate kinase (SA2220, 3.25-fold), glycerol diffusional facilitator (*glpF*, SA1140, 5.58-fold), and aerobic glycerol-3-phosphate dehydrogenase (*glpD*, SA1142, 5.45-fold). *glpD* is known to be induced by glycerol and repressed by glucose (14). Consistent with the model for expression of glycerol-3-phosphate dehydrogenase for *Bacillus subtilis* (22), the glycerol uptake operon antiterminator regulatory protein (*glpP*, SA1139, 2.1-fold) was also up-regulated in the *hemB* mutant compared to the parental strain. While a regulatory linkage in *B. subtilis* between antitermination by GlpP and the phosphoenolpyruvate:sugar phosphotransferase system (PTS) was described, phosphoenolpyruvate-protein phosphatase (*ptsI*, SA0935), one of the two major proteins of the PTS, was found to be down-regulated in the *hemB* mutant compared to its parental strain (0.59-fold). Of interest, a murine model revealed that an *S. aureus* ΔptsI mutant had a 10-fold-higher 50% lethal dose than its virulent wild-type strain did (13).

Pyruvate as well as intra- and extracellular lactate also oc-

curred as a reporter metabolite (Fig. 3). Here, significant changes occurred in the expression of both lactate dehydrogenases, which catalyze the reversible NAD-dependent interconversion of pyruvate to L-lactate, representing the final step in anaerobic glycolysis of lactic acid bacteria. The gene for the anaerobic L-lactate dehydrogenase (*lctE*, SA0232) revealed a dramatically increased expression (40.16-fold up-regulated in the *hemB* mutant in comparison of pooled values), while the aerobic L-lactate dehydrogenase (SA2395) was down-regulated. This observation of an anaerobic metabolism occurring in the *hemB* mutant is in line with earlier indications that principally fermentative pathways are activated in the *hemB* mutant (7). The massive up-regulation of the anaerobic L-lactate dehydrogenase in the *hemB* mutant is obviously required for terminal oxidation of NADH. Simultaneously, the gene encoding a lactate importer (*lctP*, SA0106) showed a reduced expression level in the mutant, the reason for which remains elusive.

In contrast to the parental strain, the *hemB* mutant shows a lower level of acetate utilization (12). Accordingly, transcriptional differences in acetate metabolism were found: with the exception of the pyruvate oxidase (*pox*, SA2327), genes from pathways leading to acetate were significantly down-regulated in the *hemB* mutant (Fig. 3). Pyruvate oxidase utilizes P_i to produce acetyl-P (oxygen dependent), which in turn produces ATP and acetate. The up-regulation of pyruvate oxidase can be considered a clear benefit for the energy-starved *hemB* mutant.

Despite the increased expression of genes belonging to lower glycolysis and the pathway leading to lactate (Fig. 3), the gene responsible for converting phosphoenolpyruvate to pyruvate (pyruvate kinase, *pykA*, SA1520) (bridging these two aforementioned segments of increased expression) did not change its expression level at all. Here, it is conceivable that the significantly increased expression of several PTSs (among which is *ptsG* [SA2326], the PTS responsible for glucose uptake) takes over the conversion of phosphoenolpyruvate to pyruvate.

In the TCA cycle, several reporter metabolites occurred as a result of a decreased expression of aconitate hydratase (*citB*, SA1184, 0.34-fold), isocitrate dehydrogenase (*citC*, SA1517, 0.39-fold), and citrate synthase (*citZ*, SA1518, 0.42-fold). In addition, intermediate compounds produced by the pyruvate dehydrogenase and the oxoglutarate dehydrogenase complexes were identified as reporter metabolites (Fig. 2 and 3). The genes particularly contributing to this were *pdhBCD* (SA0944 to SA0946, 0.66-, 0.34-, and 0.50-fold changes, respectively), *odhAB* (dihydrolipoamide succinyltransferase, SA1244, 0.20-fold), and 2-oxoglutarate dehydrogenase E1 (SA1245, 0.26-fold). Interestingly, these differences were significant only at the time points 2 through 5, representing early-exponential through stationary growth (Fig. 2).

Purine biosynthesis. Our analysis identified several intermediates from the purine synthesis as reporter metabolites (see Fig. S1 in the supplemental material; Fig. 2). The differently regulated genes related to these metabolites were the genes of the *pur* operon (comprising *purCDEFHKLMNQ*) (SA0918, SA0926, SA1048, SA0922, SA0925, SA0917, SA0921, SA0923, SA0924, and SA0920), *folD* (FolD bifunctional protein, SA0915), and *fhs* (formyltetrahydrofolate synthetase, SA1553). All genes showed a decreased expression profile in the *hemB* mutant

compared to the parent strain (Table 2). The genes *folD* and *fhs* strictly belong to the biosynthesis of folate coenzymes, which are, however, required for purine synthesis. The analysis of the different growth phases showed that the reported genes are down-regulated only up to mid-log phase (time points 1 to 3, Fig. 2), while at the late exponential and stationary phases of growth no difference between the *hemB* mutant and its parental strain was detected. Fisher's exact test confirmed these findings for pooled values and lag through logarithmic phase as given in Table 3.

In *B. subtilis*, a regulator protein, PurR (*S. aureus* homologue SA0454), was found to repress *purA* (adenylosuccinate synthase, *S. aureus* homologue SA0016), *glyA* (serine hydroxymethyl transferase, *S. aureus* homologue SA1915), *folD*, and the complete *pur* operson (8). In *Lactococcus lactis*, an activator homologous to the *B. subtilis purR* repressor was identified (11). We found that expression of staphylococcal *purR* was only slightly elevated in the *hemB* mutant in contrast to its wild-type progenitor strain (1.45-fold). The reason for the significant down-regulation of purine synthesis remains unknown.

Membrane bioenergetics. The phenotype of hemin-auxotroph SCVs is likely linked to disruption of electron transport (25, 36). Consistent with this idea, all of the genes involved in membrane bioenergetics were found to be overrepresented in the combined analysis and in the stationary growth phase if analyzed on its own. Affected genes were the NADH dehydrogenase subunit (*ndhF*, SA0411, 5.0-fold), cytochrome *d* ubiquinol oxidase subunit II homologue (SA0937, 2.13-fold), hypothetical protein similar to ferredoxin oxidoreductase beta subunit (SA1132, 2.34-fold), cytochrome *d* ubiquinol oxidase subunit I homologue (SA0937, 2.14-fold), hypothetical protein similar to thioredoxin reductase (SA1311, 2.12-fold), and ferredoxin (*fer*, SA1315, 2.31-fold).

Cell division and cell wall synthesis. *S. aureus* SCVs show impaired cell separation and incomplete or multiple cell walls (10). Genes involved in these processes were found to be up-regulated in the *hemB* mutant, for example, *pbpA* (penicillin-binding protein 1, SA1024, 2.4-fold), *llm* (lipophilic protein affecting bacterial lysis rate and methicillin resistance, SA0702, 2.2-fold), *pbp2* (penicillin-binding protein 2, SA1283, 2.4-fold), and *varS* (two-component sensor histidine kinase, SA1701, 4.09-fold). VarS has been described as a sensor critical for the control of penicillin-binding proteins (38). This protein may play a major role in the alteration of expression of genes involved in cell wall synthesis and cell division and, therefore, may contribute to the reduced susceptibility of the *hemB* mutant to antimicrobial agents.

CPs and adhesions. The role of the *S. aureus* capsule in the pathogenesis of staphylococcal infections has been investigated in several animal models of infection. Of interest, we found that the genes for capsular polysaccharide (CP) synthesis, *capA*, *capB*, *capC*, *capD*, *capE*, *capF*, and *capG* (SA0144 to SA0150), were up-regulated in the *hemB* mutant compared to the parent strain, especially at the lag phase and early logarithmic phase. The group of genes for "adaptation to atypical conditions," which includes the genes encoding proteins responsible for capsular polysaccharide synthesis, were found to be overrepresented at lag phase and early logarithmic phase and also if values for all growth phases were pooled (Table 3). These findings correlate with a previous study demonstrating

growth-dependent expression of CPs (23). While CPs have been shown to enhance virulence in animal models of staphylococcal pathogenesis, antithetically they have been found to reduce an early step in infection, bacterial adherence (32, 33). However, our microarray experiments showed that when expression of genes for CPs was reduced, expression of genes for adhesions was increased (e.g., fibrinogen-binding protein A [clfA, SA0742, 4.74-fold up-regulated in hemB mutant at early logarithmic growth phase] and clumping factor B [clfB, SA2423, 2.96-fold up-regulated in hemB mutant at logarithmic growth phase]). Since adhesion to host cells represents the precursor step to internalization for the bacteria within host cells (5, 21), it may be assumed that up-regulation of genes coding for adhesions may increase the hemB mutant's ability to invade and persist intracellularly.

In summary, while previously detected single genomic traits of the S. aureus hemB mutant were confirmed by this approach, this full-genome microarray also offered a more complete genomic analysis of the hemB mutant and provided insight into the expression profile. Profound differences were identified especially in the purine biosynthesis as well as in the arginine and proline metabolism. Of particular interest, a hypothetical gene of the Crp/Fnr family (SA2424), being part of the AD pathway, whose homologue in Streptococcus suis is assumed to be involved in intracellular persistence, showed a significantly increased transcription in the hemB mutant. The hemB mutant potentially uses the up-regulated AD pathway to produce ATP or (through ammonia production) to counteract the acidic environment that prevails intracellularly. The metabolic rearrangements may be responsible for the association of SCVs with chronic and persistent infections. Furthermore, genes involved in capsular polysaccharide and cell wall synthesis were found to be significantly up-regulated in the hemB mutant and thus potentially responsible for the changed cell morphology of SCVs and its consequences. Further work, however, is necessary to decipher the regulatory program of the SCV phenotype.

REFERENCES

1. **Baumert, N., C. von Eiff, F. Schaaff, G. Peters, R. A. Proctor, and H. G. Sahl.** 2002. Physiology and antibiotic susceptibility of Staphylococcus aureus small colony variants. Microb. Drug Resist. **8:**253–260.
2. **Casiano-Colón, A., and R. E. Marquis.** 1988. Role of the arginine deiminase system in protecting oral bacteria and an enzymatic basis for acid tolerance. Appl. Environ. Microbiol. **54:**1318–1324.
3. **Cheung, A. L., A. S. Bayer, G. Zhang, H. Gresham, and Y. Q. Xiong.** 2004. Regulation of virulence determinants in vitro and in vivo in Staphylococcus aureus. FEMS Immunol. Med. Microbiol. **40:**1–9.
4. **Degnan, B. A., M. C. Fontaine, A. H. Doebereiner, J. J. Lee, P. Mastroeni, G. Dougan, J. A. Goodacre, and M. A. Kehoe.** 2000. Characterization of an isogenic mutant of Streptococcus pyogenes Manfredo lacking the ability to make streptococcal acid glycoprotein. Infect. Immun. **68:**2441–2448.
5. **Dziewanowska, K., J. M. Patti, C. F. Deobald, K. W. Bayles, W. R. Trumble, and G. A. Bohach.** 1999. Fibronectin binding protein and host cell tyrosine kinase are required for internalization of Staphylococcus aureus by epithelial cells. Infect. Immun. **67:**4673–4678.
6. **Gruening, P., M. Fulde, P. Valentin-Weigand, and R. Goethe.** 2006. Struc-
ture, regulation, and putative function of the arginine deiminase system of Streptococcus suis. J. Bacteriol. **188:**361–369.
7. **Heinemann, M., A. Kummel, R. Ruinatscha, and S. Panke.** 2005. In silico genome-scale reconstruction and validation of the Staphylococcus aureus metabolic network. Biotechnol. Bioeng. **92:**850–864.
8. **Johansen, L. E., P. Nygaard, C. Lassen, Y. Agerso, and H. H. Saxild.** 2003. Definition of a second Bacillus subtilis pur regulon comprising the pur and xpt-pbuX operons plus pbuG, nupG (yxjA), and pbuE (ydhL). J. Bacteriol. **185:**5200–5209.
9. **Jonsson, I. M., C. von Eiff, R. A. Proctor, G. Peters, C. Ryden, and A. Tarkowski.** 2003. Virulence of a hemB mutant displaying the phenotype of a Staphylococcus aureus small colony variant in a murine model of septic arthritis. Microb. Pathog. **34:**73–79.
10. **Kahl, B. C., G. Belling, R. Reichelt, M. Herrmann, R. A. Proctor, and G. Peters.** 2003. Thymidine-dependent small-colony variants of Staphylococcus aureus exhibit gross morphological and ultrastructural changes consistent with impaired cell separation. J. Clin. Microbiol. **41:**410–413.
11. **Kilstrup, M., and J. Martinussen.** 1998. A transcriptional activator, homologous to the Bacillus subtilis PurR repressor, is required for expression of purine biosynthetic genes in Lactococcus lactis. J. Bacteriol. **180:**3907–3916.
12. **Kohler, C., C. von Eiff, G. Peters, R. A. Proctor, M. Hecker, and S. Engelmann.** 2003. Physiological characterization of a heme-deficient mutant of Staphylococcus aureus by a proteomic approach. J. Bacteriol. **185:**6928–6937.
13. **Kok, M., G. Bron, B. Erni, and S. Mukhija.** 2003. Effect of enzyme I of the bacterial phosphoenolpyruvate:sugar phosphotransferase system (PTS) on virulence in a murine model. Microbiology **149:**2645–2652.
14. **Lascelles, J.** 1978. sn-Glycerol-3-phosphate dehydrogenase and its interaction with nitrate reductase in wild-type and hem mutant strains of Staphylococcus aureus. J. Bacteriol. **133:**621–625.
15. **Lowy, F. D.** 1998. Staphylococcus aureus infections. N. Engl. J. Med. **339:**520–532.
16. **Lu, C. D., H. Winteler, A. Abdelal, and D. Haas.** 1999. The ArgR regulatory protein, a helper to the anaerobic regulator ANR during transcriptional activation of the arcD promoter in Pseudomonas aeruginosa. J. Bacteriol. **181:**2459–2464.
17. **Maghnouj, A., A. Abu-Bakr, S. Baumberg, V. Stalon, and W. C. Vander.** 2000. Regulation of anaerobic arginine catabolism in Bacillus licheniformis by a protein of the Crp/Fnr family. FEMS Microbiol. Lett. **191:**227–234.
18. **Maghnouj, A., T. F. de Sousa Cabral, V. Stalon, and W. C. Vander.** 1998. The arcABDC gene cluster, encoding the arginine deiminase pathway of Bacillus licheniformis, and its activation by the arginine repressor argR. J. Bacteriol. **180:**6468–6475.
19. **Moisan, H., E. Brouillette, C. L. Jacob, P. Langlois-Begin, S. Michaud, and F. Malouin.** 2006. Transcription of virulence factors in Staphylococcus aureus small-colony variants isolated from cystic fibrosis patients is influenced by SigB. J. Bacteriol. **188:**64–76.
20. **Patil, K. R., and J. Nielsen.** 2005. Uncovering transcriptional regulation of metabolism by using metabolic network topology. Proc. Natl. Acad. Sci. USA **102:**2685–2689.
21. **Peacock, S. J., T. J. Foster, B. J. Cameron, and A. R. Berendt.** 1999. Bacterial fibronectin-binding proteins and endothelial cell surface fibronectin mediate adherence of Staphylococcus aureus to resting human endothelial cells. Microbiology **145:**3477–3486.
22. **Persson, M., E. Glatz, and B. Rutberg.** 2000. Different processing of an mRNA species in Bacillus subtilis and Escherichia coli. J. Bacteriol. **182:**689–695.
23. **Pöhlmann-Dietze, P., M. Ulrich, K. B. Kiser, G. Doring, J. C. Lee, J. M. Fournier, K. Botzenhart, and C. Wolz.** 2000. Adherence of Staphylococcus aureus to endothelial cells: influence of capsular polysaccharide, global regulator agr, and bacterial growth phase. Infect. Immun. **68:**4865–4871.
24. **Proctor, R. A., B. Kahl, C. von Eiff, P. E. Vaudaux, D. P. Lew, and G. Peters.** 1998. Staphylococcal small colony variants have novel mechanisms for antibiotic resistance. Clin. Infect. Dis. **27**(Suppl. 1)**:**S68–S74.
25. **Proctor, R. A., and G. Peters.** 1998. Small colony variants in staphylococcal infections: diagnostic and therapeutic implications. Clin. Infect. Dis. **27:**419–422.
26. **Proctor, R. A., C. von Eiff, B. C. Kahl, K. Becker, P. McNamara, M. Herrmann, and G. Peters.** 2006. Small colony variants: a pathogenic form of bacteria that facilitates persistent and recurrent infections. Nat. Rev. Microbiol. **4:**295–305.
27. **Roggenkamp, A., A. Sing, M. Hornef, U. Brunner, I. B. Autenrieth, and J. Heesemann.** 1998. Chronic prosthetic hip infection caused by a small-colony variant of Escherichia coli. J. Clin. Microbiol. **36:**2530–2534.
28. **Schaaff, F., G. Bierbaum, N. Baumert, P. Bartmann, and H. G. Sahl.** 2003. Mutations are involved in emergence of aminoglycoside-induced small colony variants of Staphylococcus aureus. Int. J. Med. Microbiol. **293:**427–435.
29. **Senn, M. M., M. Bischoff, C. von Eiff, and B. Berger-Bächi.** 2005. σB activity in a Staphylococcus aureus hemB mutant. J. Bacteriol. **187:**7397–7406.
30. **Sifri, C. D., A. Baresch-Bernal, S. B. Calderwood, and C. von Eiff.** 2006. Virulence of Staphylococcus aureus small colony variants in the Caenorhabditis elegans infection model. Infect. Immun. **74:**1091–1096.

31. **Spiro, S.** 1994. The FNR family of transcriptional regulators. Antonie Leeuwenhoek **66:**23–36.

32. **Thakker, M., J. S. Park, V. Carey, and J. C. Lee.** 1998. *Staphylococcus aureus* serotype 5 capsular polysaccharide is antiphagocytic and enhances bacterial virulence in a murine bacteremia model. Infect. Immun. **66:**5183–5189.

33. **Tuchscherr, L. P., F. R. Buzzola, L. P. Alvarez, R. L. Caccuri, J. C. Lee, and D. O. Sordelli.** 2005. Capsule-negative *Staphylococcus aureus* induces chronic experimental mastitis in mice. Infect. Immun. **73:**7932–7937.

34. **Vaudaux, P., P. Francois, C. Bisognano, W. L. Kelley, D. P. Lew, J. Schrenzel, R. A. Proctor, P. J. McNamara, G. Peters, and C. von Eiff.** 2002. Increased expression of clumping factor and fibronectin-binding proteins by *hemB* mutants of *Staphylococcus aureus* expressing small colony variant phenotypes. Infect. Immun. **70:**5428–5437.

35. **von Eiff, C., K. Becker, D. Metze, G. Lubritz, J. Hockmann, T. Schwarz, and G. Peters.** 2001. Intracellular persistence of *Staphylococcus aureus* small-colony variants within keratinocytes: a cause for antibiotic treatment failure in a patient with Darier's disease. Clin. Infect. Dis. **32:**1643–1647.

36. **von Eiff, C., C. Heilmann, R. A. Proctor, C. Woltz, G. Peters, and F. Götz.** 1997. A site-directed *Staphylococcus aureus hemB* mutant is a small-colony variant which persists intracellularly. J. Bacteriol. **179:**4706–4712.

37. **von Eiff, C., P. McNamara, K. Becker, D. Bates, X.-H. Lei, M. Ziman, B. R. Bochner, G. Peters, and R. A. Proctor.** 2006. Phenotype microarray profiling of *Staphylococcus aureus menD* and *hemB* mutants with the small-colony-variant phenotype. J. Bacteriol. **188:**687–693.

38. **Yin, S., R. S. Daum, and S. Boyle-Vavra.** 2006. VraSR two-component regulatory system and its role in induction of *pbp2* and *vraSR* expression by cell wall antimicrobials in *Staphylococcus aureus*. Antimicrob. Agents Chemother. **50:**336–343.